*Biosystems Engineering* (2006) **94** (3), 387–396
doi:10.1016/j.biosystemseng.2006.04.008
PM—Power and Machinery

Available online at www.sciencedirect.com
SCIENCE DIRECT®

ELSEVIER

# Using Computational Fluid Dynamics to predict Damage of a Biological Pesticide during Passage through a Hydraulic Nozzle

J.P. Fife[1]; H.E. Ozkan[2]; R.C. Derksen[3]; P.S. Grewal[4]

[1]Battelle Memorial Institute, Columbus, OH 43201, USA; e-mail of corresponding author: fifej@battelle.org
[2]Food, Agricultural, and Biological Engineering, The Ohio State University, Columbus, OH 43210, USA; e-mail: ozkan.2@osu.edu
[3]USDA – Agricultural Research Service, Application Technology Research Unit, Wooster, OH 44691, USA; e-mail: derksen.2@osu.edu
[4]Entomology, The Ohio State University, Ohio Agricultural Research and Development Center, Wooster, OH 44691, USA;
e-mail: grewal.1@osu.edu

*(Received 6 May 2005; accepted in revised form 11 April 2006; published online 6 June 2006)*

The wide variety of agricultural spray equipment commercially available makes it difficult to test equipment components for compatibility with biological pesticides under varying operating conditions. One approach to this problem is to use computational fluid dynamics (CFD) as a tool to numerically simulate the complex flow conditions within different equipment components. From the numerical simulations, the flow-field parameter energy dissipation rate is used to characterise local hydrodynamic conditions potentially resulting in organism damage. Experimental tests measured damage to a benchmark biological pesticide, entomopathogenic nematodes (EPNs), after being passed through a standard flat fan nozzle (Spraying Systems XR8001VS) and hollow cone nozzle (Spraying Systems TXA8001VK) at varying flow rates. Numerical simulations of the internal flow for each nozzle were performed for the experimental flow conditions. An empirical model relating EPN damage as a function of the computed average energy dissipation rate was developed using data from a previous study. The model was validated using experimental and numerical results from the nozzles. Overall, the model was able to predict EPN damage well, in many cases within 5% of observed rates of damage. The results from this study show that CFD is a feasible method to evaluate spray equipment and operating conditions for delivery of biopesticides.


## 1. Introduction

The wide variety of agricultural spray equipment commercially available makes it difficult to individually test each component for compatibility with each biological pesticide under varying operating conditions. One approach to this problem is to use computational fluid dynamics (CFD) as a tool to numerically simulate the complex flow conditions within different equipment components. Important flow-field parameters from the numerical simulations can then be evaluated to determine whether the conditions within a particular equipment component are suitable to avoid hydrodynamic damage to the organisms.

Deformation of a body immersed within a fluid results from the superposition of normal and tangential forces from the flow field acting on the surface of the body (*i.e.* stresses). Mathematically, stress is described by corresponding velocity-gradient components. Energy dissipation rate is used to characterise local hydrodynamic conditions because it captures the effect of the nine velocity-gradient components into a scalar value. Practically, energy dissipation rate represents the rate of viscous energy being dissipated by the fluid element directly to a body that is in the control volume of that fluid element. Energy dissipation rate has been used by several researchers to characterise flow conditions resulting in cell (Gregoriades *et al.*, 2000; Ma *et al.*, 2002) and organism (Fife *et al.*, 2004) damage.

The concept that energy dissipation can be related to cell damage was first suggested by Bluestein and Mockros (1968), with respect to haemolysis of red blood cells. More recently, Gregoriades *et al.* (2000) sought to test the hypothesis that energy dissipation can characterise the hydrodynamic conditions within a flow field that result in cell detachment from microcarriers. Their study was unique because it was the first to combine an experimental study of cell damage with high resolution, numerical simulations of the flow field (an abrupt contraction) which created the cell damage. Encouragingly, they found that the magnitude of energy dissipation rate at which cell detachment began to be detected (1000 W/m$^3$) was comparable to the estimated maximum energy dissipation in bioreactors operated under conditions where cell detachment was observed (Venkat *et al.*, 1996).

In a similar study using a more advanced microfluidic flow device, Ma *et al.* (2002) evaluated four mammalian cell lines in suspension and found that the suspended cells were able to withstand relatively intense energy dissipation rates (10–100 MW/m$^3$). These energy dissipation levels are several orders of magnitude higher than measured maximum energy dissipation rates generated by impellers in bioreactors of approximately 0·1 MW/m$^3$ (Wernersson & Tragardh, 1999; Zhou & Kresta, 1996). The quantitative results of Ma *et al.* (2002), which indicate the robustness of these cells, reflect the successful culturing of mammalian cells observed in practice using large-scale bioreactors. Based on the above discussion, energy dissipation rate is a meaningful parameter to characterise the damaging effects of a flow field on a biological material.

Using methods similar to Gregoriades *et al.* (2000), Fife *et al.* (2004) have extended the body of knowledge to include the effects of hydrodynamics on entomopathogenic nematodes (EPNs), a biological pest control agent. Fife *et al.* (2004) found that appreciable damage to EPNs occurred at energy dissipation rates ranging between 120 MW/m$^3$ and 370 MW/m$^3$, which is comparable to the levels reported by Ma *et al.* (2002) for suspended cells. More interestingly, there is a clear trend in the damage response of the EPNs with respect to increases in energy dissipation rate, which was also observed in the studies for mammalian cells (Gregoriades *et al.*, 2000; Ma *et al.*, 2002). The relative damage remains low until a certain level of energy dissipation rate, and then increases rapidly toward 100% at higher levels. The consistency in the relationship between relative damage and energy dissipation rate, termed sigmoid, provided incentive to model the relationship using an empirical function.

Therefore, the overall goal of this study was to determine the feasibility of using CFD to predict the suitability of an equipment component for safe delivery of a benchmark biological pesticide, entomopathogenic nematodes. The specific objectives of this study were: (1) to develop an empirical model describing the relationship between EPN damage and energy dissipation rate using data from a previous study (Fife *et al.*, 2004); and (2) to predict EPN damage after flow through two common agricultural spray nozzles (standard flat fan and hollow cone) using computed energy dissipation rates from numerical simulations of the nozzles as input for the mathematical model.

## 2. Materials and methods

### 2.1. *Approach*

The relationship between EPN damage and energy dissipation rate was described using an empirical model. The EPN damage after exposure to the experimental flow field was measured and the energy dissipation rate was computed from CFD simulations of the experimental flow field.

The creation and evaluation of the empirical model occurred in two separate parts. Firstly data that were generated in a previous study (Fife *et al.*, 2004) were used to create the model. In the Fife *et al.* (2004) study, the experimental flow field was an abrupt contraction. Secondly, the model was evaluated (or verified) using the determined model parameter estimates and data from a separate study. In this case, the data used in the model evaluation were generated from the experimental flow fields of a standard flat fan and hollow cone spray nozzle. Thus, the model was developed and then evaluated using data generated under different experimental conditions.

### 2.2. *Experimental tests*

A comprehensive description of the experimental tests has previously been reported by Fife *et al.* (2005). Briefly, four species of EPNs were studied: *Heterorhabditis bacteriophora* (Poinar) GPS 11 strain, *Heterorhabditis megidis* (Poinar, Jackson and Klein) UK strain, *Steinernema carpocapsae* (Weiser) All strain, and *Steinernema glaseri* (Steiner) NJ strain. The EPNs were cultured *in vivo* in the laboratory using last-instar *Galleria mellonella* (L.) (Vanderhorst Canning Co., St. Marys, OH) as the host and standard culture procedures (Kaya & Stock, 1997). All tests were conducted within 2 weeks following harvest. For each test suspension, the relative viability of three 100 μ*l* subsamples was evaluated prior to testing and served as a control. The overall relative viability of control suspensions was 99·2% (standard error, SE of 0·2%).

The experiments were conducted using an opposed-pistons flow device developed by Clay and Koelling

(1997). The device consists of two high-pressure pipes (stainless steel, diameter 14·5 mm, length 355·6 mm) (High Pressure Equipment, Erie, PA) that are coupled with an orifice plate (stainless steel, orifice diameter 14·5 mm, plate thickness 1·8 mm). A stainless-steel gasket was specially made to hold the plastic casing of the nozzle within the orifice plate opening. Two pistons (stainless steel, diameter 14·4 mm, stroke length 304·8 mm) (High Pressure Equipment, Erie, PA) are moved in phase by a hydraulic system, so that as one piston moves forward, forcing the suspension through the pipe and the nozzle, the other piston retracts on the collection side. Prior to each test, the piston speed was measured using a digital tachometer (DT-107, Shimpo, Japan), and any adjustments to the piston speed were made at this time. All tests were within 0·4 mm/s (SE = 0·02 mm/s) of the desired piston speed.

Two hydraulic nozzles were evaluated in this study: flat fan (Spraying Systems XR8001VS, Spraying Systems Co., Wheaton, IL) and hollow cone (Spraying Systems TXA8001VK). Prior to conducting the individual tests, the EPN suspensions were thoroughly mixed and approximately 50 m*l* of the suspension was loaded into the pipe, between the piston and the nozzle. The total time for running each test was less than 10 min. Tests were conducted at piston speeds of 130, 170, and 210 mm/s for each nozzle, and 250 mm/s (only flat fan nozzle); corresponding to volumetric flow rates of 21·5, 28·1, 34·7, and 41·3 m*l*/s, respectively. Tests at each flow rate were repeated two times. Treatment order was not randomised.

## 2.3. *Quantification of nematode damage*

Nematode damage was quantified following the procedure of Fife *et al.* (2003). Three 100 μ*l* subsamples per replication were counted for all treatments. Nematode damage was determined by separately recording the number of live $N_L$, dead $N_D$, half pieces $N_{HP}$, and quarter pieces $N_{QP}$ of nematodes within a subsample. Nematodes were considered dead if they were broken or did not respond to prodding. The relative damage of EPNs $D_R$ in % after treatment was computed by the following equation:

$$D_R = 100 - \left(\frac{N_L}{N_L + N_D + (N_{HP}/2) + (N_{QP}/4)}\right) \times 100 \quad (1)$$

## 2.4. *Numerical Simulations*

A detailed description of the development of the computer simulation models has previously been reported by Fife *et al.* (2005). The internal flow fields of the XR8001VS flat fan and TXA8001VK hollow cone nozzles were simulated using FLUENT (Version 6·0, FLUENT, Inc., Lebanon, NH). The grid meshes used in the FLUENT simulations for the flat fan and hollow cone nozzles are presented in *Figs 1* and *2*, respectively.

Simulations of the flow field of each nozzle were conducted for each of the experimental flow rates. A user-defined function was created in FLUENT to compute the energy dissipation rate from the flow field information. The rate of viscous energy dissipated

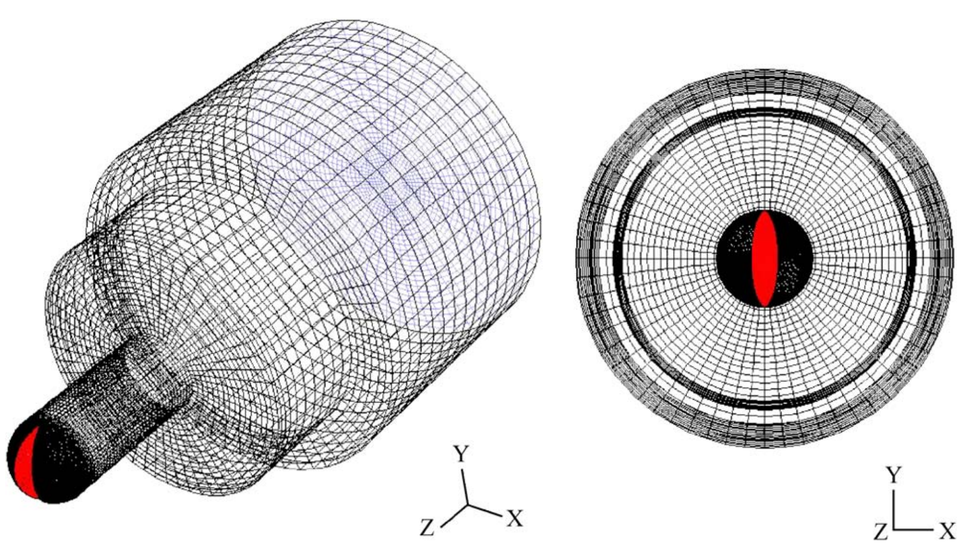


*Fig. 1. Grid mesh of XR8001VS flat fan nozzle used in FLUENT to simulate experimental flow field*

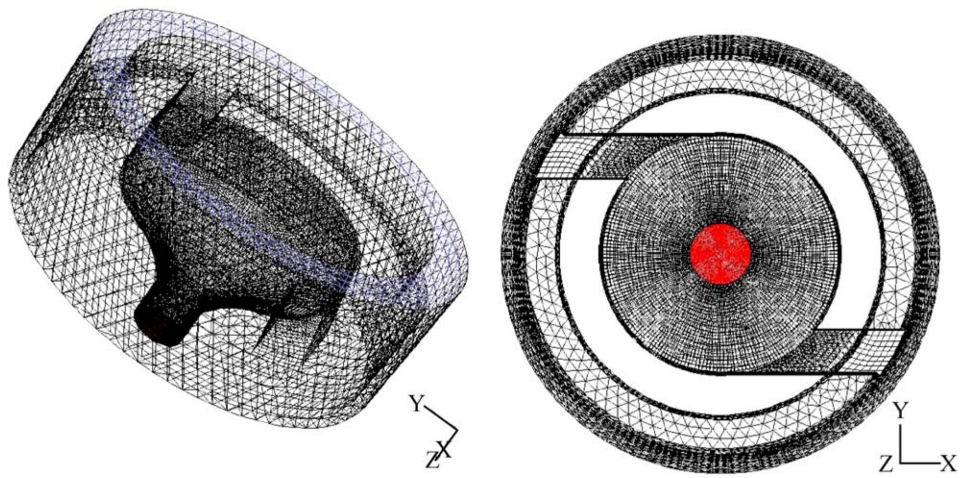


*Fig. 2. Grid mesh of TXA8001VK hollow cone nozzle used in FLUENT to simulate experimental flow field*

$\mathrm{d}Q_f/\mathrm{d}t$ in W per unit of volume $\Delta V$ in $m^3$ for three-dimensional flow is computed by the following equation (Schlichting, 1955),

$$\frac{\mathrm{d}Q_f}{\mathrm{d}t\,\Delta V} = \mu\left[2\left(\frac{\partial u_x^2}{\partial x} + \frac{\partial u_y^2}{\partial y} + \frac{\partial u_z^2}{\partial z}\right) + \left(\frac{\partial u_y}{\partial x} + \frac{\partial u_x}{\partial y}\right)^2 + \left(\frac{\partial u_z}{\partial y} + \frac{\partial u_y}{\partial z}\right)^2 + \left(\frac{\partial u_z}{\partial x} + \frac{\partial u_x}{\partial z}\right)^2\right] \quad (2)$$

where: $\mu$ is the fluid viscosity in kg/m s; and $u_x$, $u_y$, and $u_z$ are the velocity components in m/s in the X, Y, and Z directions with coordinates in m, respectively. It was assumed that all the viscous energy being dissipated by the fluid element would be fully realised by the organism. The average energy dissipation rate from within the exit orifice region was determined for each nozzle and for each experimental condition.

### 2.5. *Mathematical model development*

From Fife *et al.* (2004), the average energy dissipation rates within an abrupt contraction that were computed in FLUENT and the corresponding observed nematode relative damage after flow through the contraction provided the data for development of an empirical model. On observation, the experimental nematode damage increases in a sigmoidal fashion from 0% to near 100% with increases in energy dissipation rate for each of the EPN species. Thus, two models whose curves are both sigmoid were evaluated: the logistic model and the Gompertz model (Batschelet, 1976).

The logistic model is defined by the following equation,

$$y_{RD} = \frac{a_L}{1 + \exp(-(b_L + c_L x_{EDR}))} \quad (3)$$

where: $y_{RD}$ is the model predicted nematode relative damage in %; $x_{EDR}$ is the model input average energy dissipation rate from FLUENT simulations in W/m$^3$; and $a_L$, $b_L$, and $c_L$ are model parameters.

The Gompertz model is defined by the following equation:

$$y_{RD} = a_G \exp(-b_G \mathrm{e}^{-c_G x_{EDR}}) \quad (4)$$

where: $a_G$, $b_G$, and $c_G$ are model parameters.

In the cases of both models, parameter $a$ scales the maximum value to which the function is asymptotic, $b$ is a positioning parameter, and $c$ is a rate parameter. Parameter estimates $b_L$ and $c_L$ for the logistic model [Eqn (3)] and $b_G$ and $c_G$ for the Gompertz model [Eqn (4)] were determined in MATLAB (Version 6·0, The Mathworks, Inc., Natick, MA) using non-linear least-squares data fitting by the Gauss–Newton method. Parameters $a_L$ and $a_G$ were set to 100 because the maximum EPN damage that is possible is 100%. The parameter estimates were individually calibrated for each of the EPN species. The sum of squares of the residuals between the model and the observed relative damage values was computed for each calibrated model and was used as a measure to compare the two models.

### 2.6. *Nematode damage predictions*

The nematode relative damage after flow through each nozzle was predicted for each of the EPN species using the calibrated mathematical model that was determined to be most appropriate in the model development. The average energy dissipation rates from within the exit orifice regions of each nozzle were computed in FLUENT and were input to the mathematical model for each of the experimental conditions.

The experimental conditions and average energy dissipation rates computed in FLUENT are listed in Table 1.

The adequacy of the mathematical models to predict the independent nematode relative damage data was assessed by regression of the experimental observations onto the model predictions. A variance ratio ($F$) statistic (Dent & Blackie, 1979) that tests the regression intercept and slope simultaneously was used to determine whether the models were statistically indistinguishable from the data. This statistic follows the $F$ distribution with 2 and $n-2$ degrees of freedom, and tests the null hypothesis that the regression intercept and slope are equivalent to 0·0 and 1·0, respectively. The critical $F$ value for 2 and 2 degrees of freedom ($n = 4$) is 19, and for 2 and 1 degrees of freedom ($n = 3$) is 200. Consequently, small values of $F$ indicate that the model provides a good fit to the data.

## 3. Results

### 3.1. *Mathematical model calibration*

Tables 2 and 3 list the model parameter estimates $a_L$, $b_L$, and $c_L$ for the logistic model [Eqn (3)] and $a_G$, $b_G$, and $c_G$ for the Gompertz model [Eqn (4)] that were calibrated, along with the sum of squares of the residuals, for each of the EPN species, respectively. The model computed and the observed mean nematode relative damage after treatment with the abrupt contraction as a function of the average energy dissipation rates computed in FLUENT (Fife *et al.*, 2004) are presented in *Fig. 3* for *H. bacteriophora* (a), *H. megidis* (b), *S. carpocapsae* (c) and *S. glaseri* (d) for both models. The total sum of squares (SS) of the residuals, summed over the EPN species, was lower for the Gompertz model (SS = 23 463) compared to the logistic model (SS = 25 247). Thus, the Gompertz model was selected for further analysis and is referred to as 'the model' in the remainder of the study.

**Table 1**
**Average energy dissipation rates computed in FLUENT for flow through XR8001VS flat fan nozzle and TXA8001VK hollow cone nozzle for range of experimental conditions**

| *Volumetric flow rate, ml/s* | *Average energy dissipation rate, MW/m³* | |
|---|---|---|
| | *XR8001VS* | *TXA8001VK* |
| 21·5 | 110 | 5·10 |
| 28·1 | 187 | 6·97 |
| 34·7 | 285 | 9·10 |
| 41·3 | 402 | —* |

*Experimental flow rate not tested for TXA8001VK.

### 3.2. *Nematode damage predictions*

The average energy dissipation rates listed in Table 1 for each nozzle were input to the Gompertz model [Eqn (4), Table 3] for each of the EPN species. The resulting model predictions of nematode relative damage and the corresponding observed mean nematode relative damage after flow through the XR8001VS flat fan and TXA8001VK hollow cone nozzles are presented in *Figs 4 and 5*, respectively, for *H. bacteriophora* (a), *H. megidis* (b), *S. carpocapsae* (c), and *S. glaseri* (d), for each of the experimental conditions.

Tables 4 and 5 provide a summary of the sum of squares of the residuals and the regression of the observed mean nematode relative damage onto the model predictions for each of the EPN species for the XR8001VS flat fan and TXA8001VK hollow cone nozzles. Tables 6 and 7 list the percent differences between the model predictions and experimental observations for each of the experimental conditions.

For XR8001VS, the Gompertz model was statistically acceptable in predicting the independent nematode

**Table 2**
**Logistic model parameter estimates $a_L$, $b_L$, and $c_L$ and 95% confidence intervals calibrated for *Heterorhabditis bacteriophora*, *Heterorhabditis megidis*, *Steinernema carpocapsae*, and *Steinernema glaseri***

| *Entomopathogenic nematode species* | *Logistic model parameter estimates** | | | | |
|---|---|---|---|---|---|
| | $a_L$ | $b_L$ | $b_L$ 95% confidence interval | $c_L$ | $c_L$ 95% confidence interval |
| *H. bacteriophora* | 100 | –2·7294 | –0·6342 | $9{\cdot}6912 \times 10^{-9}$ | $2{\cdot}3200 \times 10^{-9}$ |
| *H. megidis* | 100 | –7·7327 | –2·2302 | $3{\cdot}1882 \times 10^{-8}$ | $0{\cdot}9195 \times 10^{-8}$ |
| *S. carpocapsae* | 100 | –4·4299 | –0·5774 | $7{\cdot}0246 \times 10^{-9}$ | $1{\cdot}0675 \times 10^{-9}$ |
| *S. glaseri* | 100 | –5·9321 | –1·2838 | $2{\cdot}1154 \times 10^{-8}$ | $0{\cdot}4565 \times 10^{-8}$ |

*Model calibrations conducted using experimental data from a previous study using an abrupt contraction (Fife *et al.*, 2004). Average energy dissipation rates within the abrupt contraction computed in FLUENT for each of the experimental conditions were input for the model calibration. Model output was compared to observed nematode relative damage to determine the best fitting model parameters according to the Gauss–Newton method. ($n = 60$, except for *S. glaseri* $n = 24$).

**Table 3**
**Gompertz model parameter estimates $a_G$, $b_G$, and $c_G$ and 95% confidence intervals calibrated for *Heterorhabditis bacteriophora*, *Heterorhabditis megidis*, *Steinernema carpocapsae*, and *Steinernema glaseri***

| *Entomopathogenic nematode species* | *Gompertz model parameter estimates** | | | | |
|---|---|---|---|---|---|
| | $a_G$ | $b_G$ | $b_G$ 95% confidence interval | $c_G$ | $c_G$ 95% confidence interval |
| *H. bacteriophora* | 100 | 3·9838 | 1·3504 | $6{\cdot}5410 \times 10^{-9}$ | $1{\cdot}4070 \times 10^{-9}$ |
| *H. megidis* | 100 | 26·1589 | 22·4402 | $1{\cdot}5191 \times 10^{-8}$ | $0{\cdot}3681 \times 10^{-8}$ |
| *S. carpocapsae* | 100 | 7·4334 | 2·0156 | $3{\cdot}7275 \times 10^{-9}$ | $0{\cdot}5655 \times 10^{-9}$ |
| *S. glaseri* | 100 | 25·6634 | 13·1104 | $1{\cdot}3038 \times 10^{-8}$ | $0{\cdot}1868 \times 10^{-8}$ |

*Model calibrations conducted using experimental data from a previous study using an abrupt contraction (Fife *et al.*, 2004). Average energy dissipation rates within the abrupt contraction computed in FLUENT for each of the experimental conditions were input for the model calibration. Model output was compared to observed nematode relative damage to determine the best-fitting model parameters according to the Gauss–Newton method ($n = 60$, except for *S. glaseri* $n = 24$).

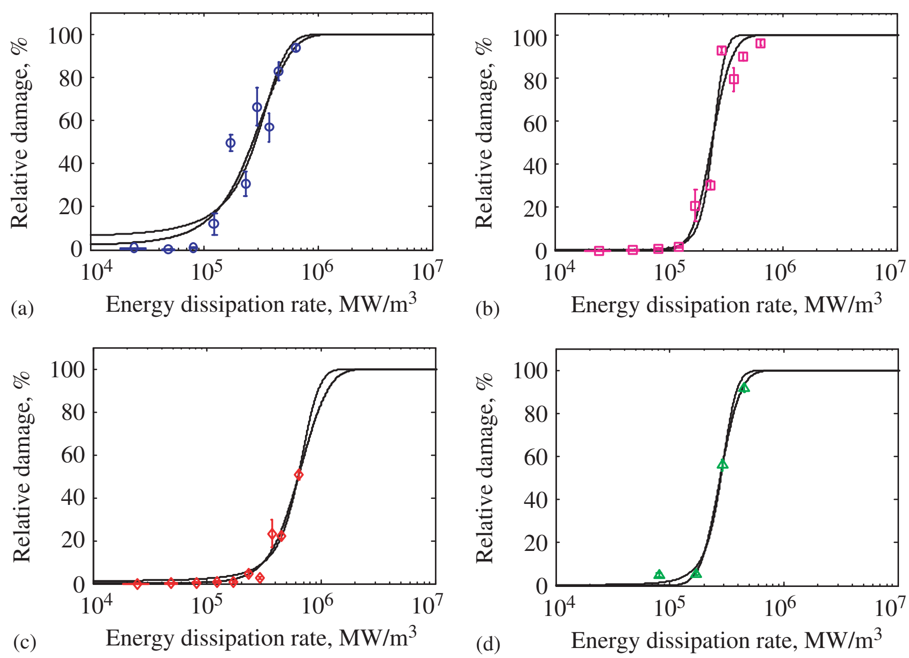


*Fig. 3. Logistic (—) and Gompertz (▬) model calibration results for (a) Heterorhabditis bacteriophora; (b) Heterorhabditis megidis; (c) Steinernema carpocapsae; and (d) Steinernema glaseri; calibration data from a previous study of an abrupt contraction (Fife et al., 2004), error bars represent the standard error of the mean ($n = 6$)*

relative damage data for *H. megidis*, *S. carpocapsae*, and *S. glaseri* ($F \leqslant 1{\cdot}4$). However, for *H. bacteriophora* the model was not statistically acceptable ($F = 141$). On average, the model over-predicted the observed data by 26·1% for *H. bacteriophora* (Table 6).

For TXA8001VK, according to the $F$ statistic, the Gompertz model adequately predicted nematode relative damage for each EPN species ($F \leqslant 15{\cdot}3$). These results are consistent for *H. bacteriophora*, *H. megidis*, and *S. carpocapsae*, whose model predicted and observed mean differences were less than or equal to 3·3% (Table 7). However, for *S. glaseri*, the model predicted no relative damage for the range of experimental conditions, while in some cases considerable damage was observed.

## 4. Discussion

The logistic [Eqn (3)] and Gompertz [Eqn (4)] functions were selected because each captures the sigmoidal relationship. The main difference between

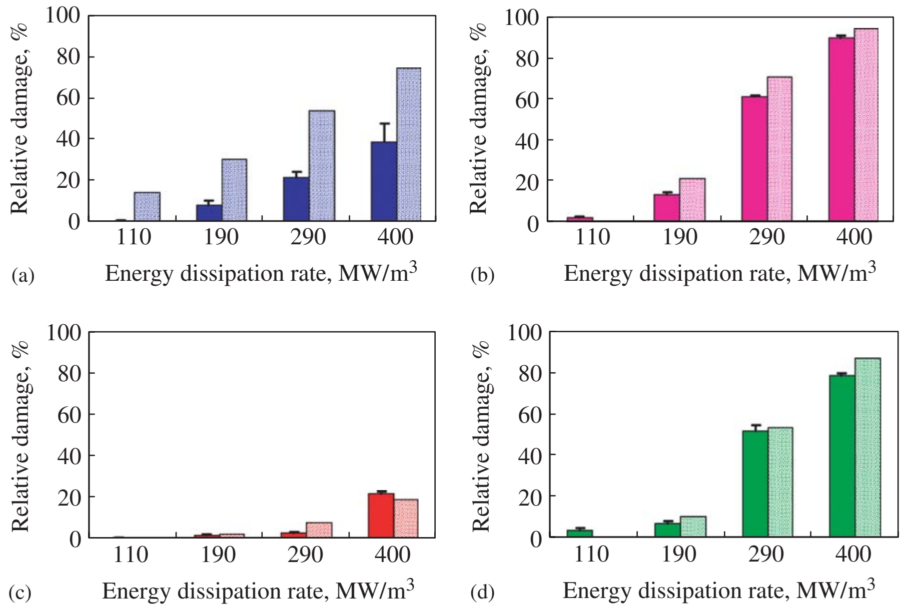


*Fig. 4. Observed mean relative damage of (a) Heterorhabditis bacteriophora; (b) Heterorhabditis megidis; (c) Steinernema carpocapsae; and (d) Steinernema glaseri after treatment with the XR8001VS flat fan nozzle, and corresponding Gompertz model predictions of nematode damage of each species, error bars represent standard error of the mean (n = 6) (data presented for range of energy dissipation rates computed in FLUENT corresponding to experimental flow rates of 21·5, 28·1, 34·7, and 41·3 ml/s)*

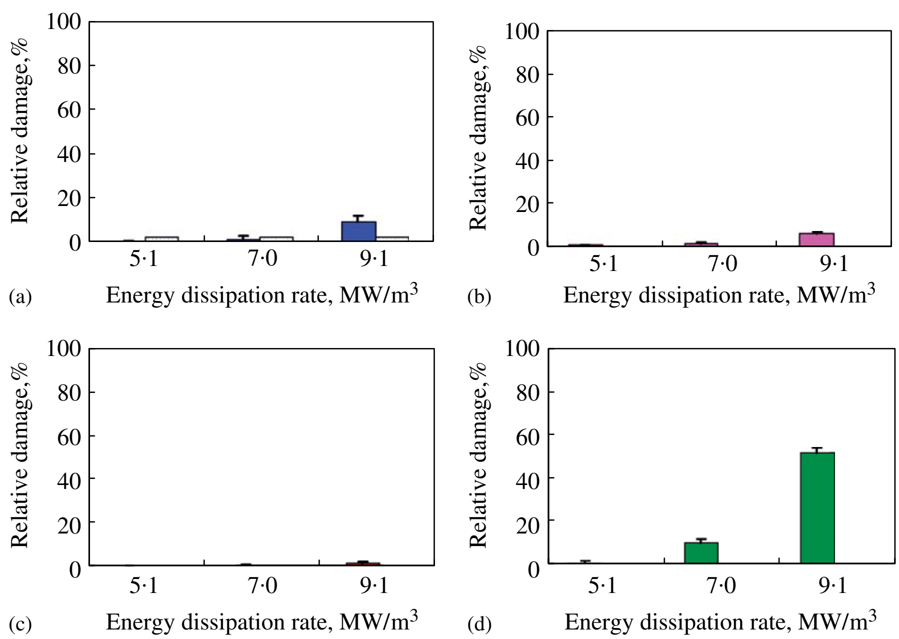


*Fig. 5. Observed mean relative damage of (a) Heterorhabditis bacteriophora; (b) Heterorhabditis megidis; (c) Steinernema carpocapsae; and (d) Steinernema glaseri after treatment with the TXA8001VK hollow cone nozzle, and corresponding Gompertz model predictions of nematode damage of each species, error bars represent standard error of the mean (n = 6) (data presented for range of energy dissipation rates computed in FLUENT corresponding to experimental flow rates of 21·5, 28·1, and 34·7 ml/s)*

these two functions is that the logistic curve is symmetrical about its central point of inflection, while the Gompertz curve is asymmetrical about its point of inflection. Thus, the derivative of the logistic function is normally distributed, while the Gompertz function derivative is skewed slightly to the right. Both functions

**Table 4**

**Summary of statistics predicting nematode relative damage using the Gompertz model for *Heterorhabditis bacteriophora*, *Heterorhabditis megidis*, *Steinernema carpocapsae*, and *Steinernema glaseri* after flow through an XR8001VS flat fan nozzle**

| *Entomopathgenic nematode species* | *Sum of Squares of Residuals*† | *Regression** | | | | |
|---|---|---|---|---|---|---|
| | | *Intercept* | *Intercept 95% confidence interval* | *Slope* | *Slope 95% confidence interval* | *F statistic*‡ |
| *H. bacteriophora* | 3016 | −10·16 | 10·65 | 0·63 | 0·22 | 141 |
| *H. megidis* | 187 | −2·70 | 18·39 | 0·94 | 0·31 | 1·2 |
| *S. carpocapsae* | 33 | −2·30 | 10·40 | 1·19 | 1·01 | 0·2 |
| *S. glaseri* | 97 | 1·37 | 11·45 | 0·90 | 0·22 | 1·4 |

*Regression of experimental observations onto model predictions.

†Sum of squares of the residuals between model predicted values [Eqn (4), Table 3] and observed mean nematode relative damages after flow through the XR8001VS flat fan nozzle ($n = 4$).

‡$F$ statistic (Dent & Blackie, 1979), the critical $F$ value is 19·00, with 2 and 2 degrees of freedom.

**Table 5**

**Summary of statistics predicting nematode relative damage using the Gompertz model for *Heterorhabditis bacteriophora*, *Heterorhabditis megidis*, *Steinernema carpocapsae*, and *Steinernema glaseri* after flow through an TXA8001VK hollow cone nozzle**

| *Entomopathgenic nematode species* | *Sum of Squares of Residuals*† | *Regression** | | | | |
|---|---|---|---|---|---|---|
| | | *Intercept* | *Intercept 95% confidence interval* | *Slope* | *Slope 95% confidence interval* | *F statistic*‡ |
| *H. bacteriophora* | 0·9 | −86·90 | 487·61 | 40·48 | 218·55 | 1·0 |
| *H. megidis* | 49 | −1·37 | 12·51 | $5{\cdot}79 \times 10^{8}$ | $1{\cdot}50 \times 10^{9}$ | 9·9 |
| *S. carpocapsae* | 42 | −9·08 | 61·22 | 131·15 | 852·25 | 0·9 |
| *S. glaseri* | 2762 | −24·51 | 92·08 | $5{\cdot}91 \times 10^{9}$ | $1{\cdot}08 \times 10^{10}$ | 15·3 |

*Regression of experimental observations onto model predictions.

†Sum of squares of the residuals between model predicted values [Eqn (4), Table 3] and observed mean nematode relative damages after flow through the TXA8001VK hollow cone nozzle ($n = 3$).

‡$F$ statistic (Dent &Blackie, 1979), the critical $F$ value is 200·00, with 2 and 1 degrees of freedom.

**Table 6**

**Differences between Gompertz model predicted and observed mean nematode relative damage of *Heterorhabditis bacteriophora*, *Heterorhabditis megidis*, *Steinernema carpocapsae*, and *Steinernema glaseri* after flow through an XR8001VS flat fan nozzle for each of the experimental conditions**

| *Energy dissipation rate, MW/m³* | *Gompertz model predicted*−Observed mean nematode relative damage*†*, %* | | | |
|---|---|---|---|---|
| | *H. bacteriophora* | *H. megidis* | *S. carpocapsae* | *S. glaseri* |
| 110 | 13·8 | −1·4 | 0·4 | −3·6 |
| 190 | 22·5 | 8·2 | 1·0 | 3·2 |
| 280 | 32·0 | 9·8 | 4·9 | 1·4 |
| 400 | 36·0 | 4·8 | −2·8 | 8·5 |
| Mean difference | 26·1 | 6·0 | 2·3 | 4·2 |

*Nematode relative damage predicted for each EPN species according to the Gompertz model [Eqn (4), Table 3].

†Nematode damage quantified by counting number of living and dead (whole and pieces) EPNs and relative damage computed according to Eqn (1).

were able to describe the calibration data well, however the Gompertz function provided a better fit to the data (*i.e.* lower sum of squares of the residuals). This is likely due to the Gompertz asymmetric sigmoid growth curve, which better captures the rapid increase in nematode relative damage at energy dissipation levels where appreciable damage starts to be observed. The Gompertz growth model has been frequently used by

**Table 7**
**Differences between Gompertz model predicted and observed mean nematode relative damage of *Heterorhabditis bacteriophora*, *Heterorhabditis megidis*, *Steinernema carpocapsae*, and *Steinernema glaseri* after flow through a TXA8001VK hollow cone nozzle for each of the experimental conditions**

| *Energy dissipation rate, $MW/m^3$* | *Gompertz model predicted*−Observed mean nematode relative damage†, %* | | | |
|---|---|---|---|---|
| | *H. bacteriophora* | *H. megidis* | *S. carpocapsae* | *S. glaseri* |
| 5·10 | 2·0 | −0·9 | 0·07 | −0·4 |
| 6·97 | 1·3 | −1·5 | 0·07 | −10·4 |
| 9·10 | −6·6 | −6·2 | −0·9 | −51·5 |
| Mean difference | 3·3 | 2·9 | 0·3 | 20·8 |

*Nematode relative damage predicted for each of the EPN species according to the Gompertz model [Eqn (4), Table 3].
†Nematode damage quantified by counting number of living and dead (whole and pieces) EPNs and relative damage computed according to Eqn (1).

ecologists to explain biological phenomena (Batschelet, 1976), and based on the above discussion this function provides a reasonable model for predicting cell or organism damage with respect to the flow field parameter energy dissipation rate.

Overall, the Gompertz model [Eqn (4), Table 3] was able to predict nematode relative damage well. For the XR8001VS flat fan, 9 out of the 12 model predictions for *H. megidis*, *S. carpocapsae*, and *S. glaseri* were within 5% of the observed nematode relative damage, and all of the model predictions were within 10%. A possible explanation for the poor model performance of *H. bacteriophora* may be the notable variance of the experimental data that was used in the model calibration [*Fig. 3*(*a*)]. The quality of the calibration data will affect the model parameter estimates that are determined using the non-linear least-squares data fitting algorithm. Additional data for *H. bacteriophora* is necessary to redefine the parameter estimates, and possibly improve the model performance.

For the TXA8001VK hollow cone, the energy dissipation rates away from the nozzle wall were considerably less than levels expected to cause damage. Thus, the Gompertz model predictions of little to no nematode damage were within 5% of the observations for most of the experimental cases. However, the model did not predict the high levels of damage observed for *S. glaseri*. As previously discussed in Fife *et al*. (2005), because of the relatively long length of *S. glaseri* nematodes with respect to the TXA8001VK exit orifice (approximately 1 mm), parts of the nematode body may have been in close proximity to the nozzle wall where energy dissipation rates were considerably higher. Near the nozzle wall, the energy dissipation rates range between 100 and 1000 $MW/m^3$ for the volumetric flow rate of 34·7 m*l*/s. The model input to predict the observed *S. glaseri* damage for this experimental condition, approximately 50%, is 280 $MW/m^3$, which is within the range of energy dissipation rates near the nozzle wall. This supports the concept discussed above and provides a meaningful explanation for the large difference between the model prediction and the observed damage for *S. glaseri*.

The robustness of the empirical model is demonstrated by the fact that not only was the model evaluated with nematode relative damage data that was independent from the model calibration, but also the two experimental systems were different. Average energy dissipation rates from the numerical simulations of an abrupt contraction were input for the model calibration, while average energy dissipation rates from the simulations of the XR8001VS flat fan and TXA8001VK hollow cone nozzles were input for the model validation.

It is important to note that selection of the most representative value of the energy dissipation rate from the flow field for input into the model is critical. Analysis of the distribution of energy dissipation values within the nozzle exit orifice showed that values remain relatively constant away from the nozzle wall. Near the nozzle wall, the energy dissipation values increase rapidly because of the assumption of no-slip at the wall (*i.e.* a large velocity gradient near the wall). Thus, it was determined that the average energy dissipation rate within the nozzle exit orifice, not including values near the wall, was the most representative value of the flow field.

The ability to successfully predict the damage response of the EPNs within different systems and under varying operating conditions shows the versatility of using energy dissipation rate as a flow-field parameter to characterise the hydrodynamic conditions responsible for the observed nematode damage. Moreover, these results show that CFD is a feasible method to evaluate the flow-field conditions within an equipment component, and provides the necessary flow-field information (*i.e.* energy dissipation rate) to predict whether or not an equipment component is suitable for a biological pesticide. This study provides a standard procedure that can be used to evaluate other equipment components and biological agents in order to develop guidelines for selection of appropriate spray equipment and operating conditions for effective application of biopesticides.

## 5. Conclusions

An empirical model was developed using data from a previous study (Fife *et al*., 2004) that related observed nematode relative damage to average energy dissipation rates within an abrupt contraction. Calibrated models for each of the entomopathogenic nematode (EPN) species were found to predict nematode damage after passage through two common agricultural nozzles (standard flat fan and hollow cone) well. Overall, 23 out of 28 model predictions were within 10% of the observed nematode relative damage, in many cases within 5%. The ability to successfully predict the damage response of the nematodes within a different system and under varying operating conditions shows the robustness of the empirical model and the versatility of energy dissipation rate to characterise the hydrodynamic conditions responsible for the nematode damage. The results from this study demonstrate the feasibility of using computational fluid dynamics (CFD) methods to evaluate the flow field within an equipment component to assess compatibility with a biological agent.

## Acknowledgements

The authors express appreciation to the following organizations for supporting this study: the Ohio Agricultural Research and Development Center (OARDC) at The Ohio State University, the USDA-ARS Application Technology Research Unit, and Spraying Systems Co. for supplying the hydraulic nozzles. Also, special thanks to Dr. J. Chalmers and Dr. K. Koelling from the Department of Chemical Engineering at The Ohio State University for use of the experimental flow device, and to A. Doklovic and D. Troyer for technical assistance in the experimental set-up.

## References

**Batschelet E** (1976). Introduction to Mathematics for Life Scientists. Springer, New York

**Bluestein M; Mockros L F** (1968). Hemolytic effects of energy dissipation in flowing blood. Medical and Biological Engineering, **7,** 1–6

**Clay J D; Koelling K W** (1997). Molecular degradation of concentrated polystyrene solutions in a fast transient extensional flow. Polymer Engineering Science, **37**(5), 789–800, doi:10.1002/pen.11722

**Dent J B; Blackie M J** (1979). Systems Simulation in Agriculture. Applied Science Publishing, London

**Fife J P; Derksen R C; Ozkan H E; Grewal P S** (2003). Effects of pressure differentials on the viability and infectivity of entomopathogenic nematodes. Biological Control, **27,** 65–72

**Fife P; Derksen R C; Ozkan H E; Grewal P S; Chalmers J J** (2004). Evaluation of a contraction flow field on hydrodynamic damage to entomopathogenic nematodes—a biological pest control agent. Biotechnology and Bioengineering, **86**(1), 96–107, doi:10.1002/bit.10879

**Fife J P; Ozkan H E; Derksen R C; Grewal P S; Krause C R** (2005). Viability of a biological pest control agent through hydraulic nozzles. Transactions of the ASAE, **48**(1), 45–54

**Gregoriades N; Clay J D; Ma N; Koelling K W; Chalmers J J** (2000). Cell damage of microcarrier cultures as a function of local energy dissipation created by a rapid extensional flow. Biotechnology and Bioengineering, **69**(2), 171–182, doi:10.1002/(SICI)1097-0290(20000720)69:2<171::AID-BIT6>3.0.CO;2-C

**Kaya H K; Stock S P** (1997). Techniques in insect nematology. In: Manual of Techniques in Insect Pathology (Lacey L A, ed), pp 281–324. Academic Press, London

**Ma N; Koelling K W; Chalmers J J** (2002). Fabrication and use of a transient contractional flow device to quantify the sensitivity of mammalian and insect cells to hydrodynamic forces. Biotechnology and Bioengineering, **80**(4), 428–437, doi:10.1002/bit.10387

**Schlichting H** (1955). Boundary Layer Theory, 2nd Edn. Pergamon Press, New York

**Venkat R V; Stock L R; Chalmers J J** (1996). Study of hydrodynamics in microcarrier culture spinner vessels: a particle tracking velocimetry approach. Biotechnology and Bioengineering, **49**(4), 456–466, doi:10.1002/(SICI)1097-0290(19960220)49:4<456::AID-BIT13>3.0.CO;2-8

**Wernersson E S; Tragardh C** (1999). Scale-up of Rushton turbine-agitated tanks. Chemical Engineering Science, **54**(19), 4245–4256, doi:10.1016/S0009-2509(99)00127-X

**Zhou G; Kresta S M** (1996). Impact of tank geometry on the maximum turbulence energy dissipation rate for impellers. AIChE Journal, **42**(9), 2476–2490, doi:10.1002/aic.690420908